Spring 2019

Optimization of Primary Cilia Detection in Musculoskeletal Tissue

Ragen Engel
ree19@zips.uakron.edu

Honors Thesis Project in Biology

Optimization of Primary Cilia Detection in Musculoskeletal Tissue

Ragen Engel, with Ashley Mohrman, PhD

Abstract

The objective of this research project was to optimize a laboratory technique for visualizing primary cilia in musculoskeletal tissue of young swine, specifically the growth plate of long bones. This was accomplished through varying fixation procedures, antigen retrieval methods, antibody concentrations, and incubation times. By varying these parameters, a reproducible procedure was developed to examine the primary cilia in multiple tissues including ligament, fascia, and growth plate. This experiment introduced variances in fixation methods, with methanol or formalin. Paraffin and frozen embedding techniques were also varied for comparison with regards to cilia visualization. Results from the acetylated alpha tubulin (aTUB) stain suggested that Paraffin-embedded tissues had a significantly greater cilia / cell ratio than frozen-embedded tissues. From a qualitative standpoint, methanol-Paraffin was proposed to be the optimal treatment method for cilia detection in growth plate tissue.

Introduction

The primary cilium is an important subcellular structure that functions as both a mechano-sensor and chemo-sensor (Moore and Jacobs 2018). Recent studies have demonstrated that these “antenna-like” structures are involved in different signaling pathways including Indian hedgehog, parathyroid hormone-related peptide, transforming growth factor, bone morphogenetic protein, fibroblast growth factor, notch, and Wnt (Moore and Jacobs 2018). It is also important to note that mutations in primary ciliary proteins can severely impact the development of musculoskeletal tissue and the ossification of bones. Further research on the structure and behavior of primary cilia can

potentially lead to a better understanding of life-altering disorders involving musculoskeletal tissue and endochondral ossification.

This experiment will focus on the articular and growth plate cartilage of the long bones. The growth plate is a region of cartilage that lies between the primary and secondary ossification centers of long bones, and allows the bones to lengthen at both ends. The growth plate, or physis, is responsible for bone elongation by chondrogenesis and endochondral ossification. The growth plate is divided into three zones; resting, proliferative and hypertrophic. The proliferative zone is composed of rapidly proliferating chondrocytes arranged in distinct columns that run along the long axis of the long bone (Garrison et al. 2017). These columns are the region of interest in this experiment as within the growth plate, primary cilia play critical roles in chondrocyte proliferation and columnar orientation (Yuan et al. 2015).

For this research project, a laboratory technique for visualizing primary cilia in musculoskeletal tissue will be optimized from published literature (McGlashan et al. 2006; Jensen et al. 2004). Immunohistochemistry (IHC) is a commonly used technique in which the specificity and high-binding capacity of antibodies are exploited to detect and locate cellular proteins *in situ*. The IHC technique follows a series of steps beginning with tissue preparation. Common fixation solutions among the cited studies include formaldehyde (or a derivative) and methanol; both will be compared in this research project (Table 1). Fixation is key to preservation

Table 1: Experimental Design

Factor	Levels	
Fixation method	Methanol	Neutral buffered formalin
Embedding technique	Frozen	Paraffin

of the tissue throughout the IHC process. This step prevents autolysis and prevents the destruction of antigens, which are necessary for fluorescent labeling with antibodies ("IHC/ICC Sample Fixation", https://www.novusbio.com/sample-fixation-for-ihc-icc). Tissues are typically embedded in paraffin or frozen. Embedding provides tissue with the support to withstand the sectioning process.

In IHC, primary and secondary antibodies are used to label target structures for detection via microscopy. The antibodies must correlate in such a way that the secondary binds to the primary, initiating indirect staining. This requires the secondary antibody to be raised against the primary. If the primary antibody had been raised in a mouse, for example, then the secondary antibody must be against the IgG of that mouse species ("Immunohistochemistry Introduction," IHCworld.com).

Experimental Methods

Section Preparation

Tissue samples were obtained from the hind-limbs of cadaveric swine with permission from the Institutional Animal Care and Use Committee of Northeast Ohio Medical University. Growth plate and articular cartilage were resected from the proximal femur, distal femur, and proximal tibia, split into 4 pieces and immediately exposed to chemical fixation overnight at 4°C. Half the samples from the resected tissue were fixed in 100% methanol and half in 10% neutral buffered formalin (NBF) to identify the preferred fixation method for viewing primary cilia (Table 1).

Samples were washed with phosphate buffered saline (PBS) and then stored in 70% ethanol at 4°C until embedding. Half the methanol-fixed samples and half the NBF

-fixed samples from each resected tissue were used in frozen embedding. The tissues were equilibrated overnight in 30% sucrose at 4°C, and then frozen in Optimal Cutting Temperature (OCT) medium and sectioned in a cryostat at 10 μm. The remaining samples from each resected tissue were used in paraffin embedding using an automated paraffin processor. Sections were cut on a microtome at 10 μm.

Staining

Paraffin slides were pre-heated at 60°C, de-paraffinized in xylene, and re-hydrated all using standard histology protocols. Frozen slides were re-hydrated in PBS. From this point, all slides were treated the same. Multiple antigen retrieval methods were tested, but proper retrieval was finally achieved by incubating slides in sodium citrate buffer (pH 6) overnight at 60°C, followed by a quick wash in PBS. A nonspecific block was then administered to prevent nonspecific antibody binding. A commercially available blocking medium, Bloxall (Vector Laboratories), remained on the slides for 1 hour.

Dual antibody staining was used to ensure primary cilia detection and avoid false discovery. Acetylated alpha-tubulin primary antibody (aTUB, Sigma # T7451) and ARL13B antibody (Protein Tech # 17711-1-AP) concentrations were first optimized for dual staining. Criteria for final concentration simply included appropriate visibility of primary cilia at the lowest concentration of each antibody. Final dilutions used for each antibody were: aTUB 1:1000 and ARL13b 1:200. The primary antibodies were incubated on the sections overnight at 4°C.

After rinsing with PBS, the secondary antibodies were applied for 1 hr at room temperature. These included Alexafluor568 goat-anti-mouse-IgG and Alexafluor488

goat-anti-rabbit-IgG (Invitrogen) which were both diluted at 1:500. Finally, nuclei were stained with Hoechst 33342, then the sections were washed and cover-slipped.

Imaging

Imaging of the primary cilia was first attempted using a multiphoton microscope (Olympus). Although cilia were visible, imaging resulted in faded cilia insufficient for measurement. After examination of the slides on a regular upright fluorescence microscope (Olympus) with a 100x oil immersion objective, we determined that standard epifluorescence could still capture the primary cilia within the cartilage tissue. Sections were all imaged using the same microscope and camera combination and keeping imaging parameters equivalent for all image capture. This includes exposure time and image averaging. Image averaging was set to a three count. Images were captured with the following exposure times for each filter: Cy3- 25 ms; GFP- 11 ms; DAPI- 0.5 ms. Image acquisition was accomplished with Image-Pro (Media Cybernetics). Images were not further processed before intensity measures were captured. However, for overlay images, contrast was enhanced to better visualize cilia.

Optimization Measures

Data was collected using ImageJ software (NIH open access) for primary cilia max intensity, cell body max intensity, and image background max intensity. Values were further analyzed in Excel. Image background was subtracted from cilia and cell body values, and then cilia intensities and cilia/body intensity ratios were compared.

Statistical Analysis

Quantitative measures, including the corrected maximum cilia intensity values, ratio of cilia max to cell body max, and quality score were analyzed using a two-factor analysis of variance (ANOVA) using $\alpha = 0.05$ in JMP software (SAS Institute).

Results

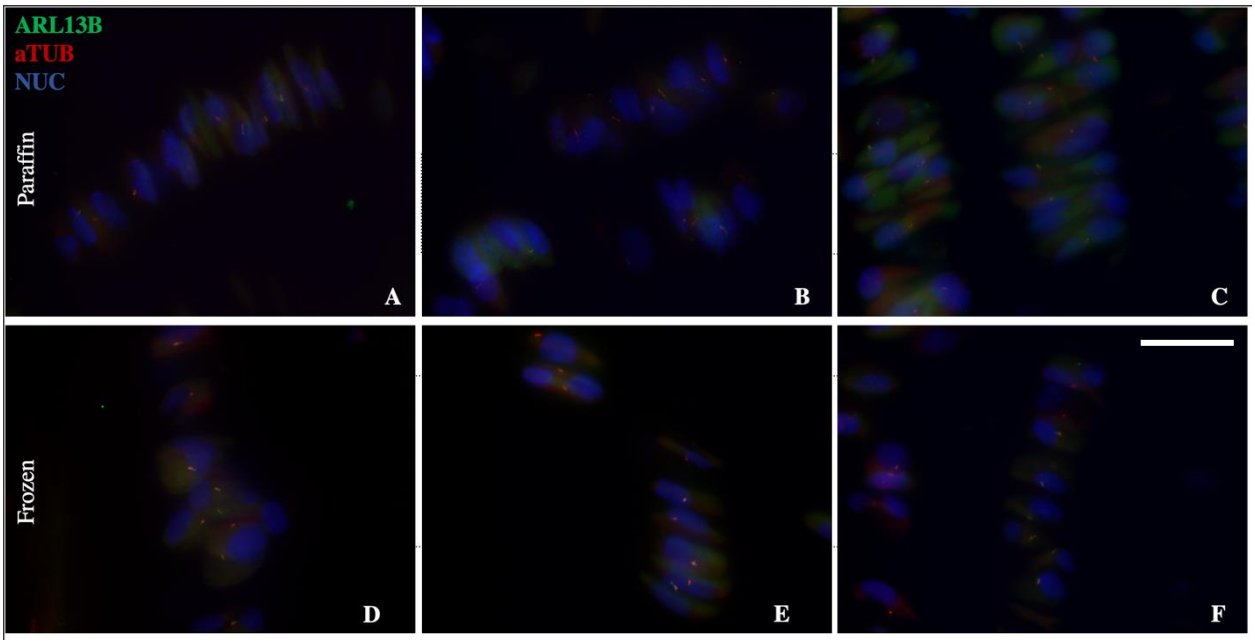

Figure 1. Methanol-fixed cartilage samples from cadaveric swine. Panels A, B, and C were obtained from samples embedded in paraffin; panels D, E, and F were obtained from samples embedded in freezing medium. Panels were generated by overlaying the original images obtained by means of three different filters; Cy3, GFP, and DAPI. Cy3 was used to visualize acetylated alpha-tubulin (aTUB) primary antibody, shown in red. GFP was utilized to screen for ARL13B antibody, dyed green. DAPI was employed to stain cell nuclei (NUC), shown in blue. Contrast was enhanced to best distinguish primary cilia. (Scale bar = 20 μm)

The methanol-fixed cartilage samples, including those embedded in paraffin and frozen medium, produced quality images of dual antibody staining (Figure 1). Cilia staining with aTUB appeared bright and prominent, projecting as small rod-like structures from the outer portion of the cell bodies. Quality of the aTUB staining seemed to vary more between sections in the methanol-frozen group than sections in the methanol-paraffin group. However, the ARL13b staining seemed to be the most evident

in the methanol-fixed groups than in the NBF-fixed groups (Figure 2). The two methanol-fixed groups presented with overall distinct nuclear, ARL13b, and aTUB staining. Qualitatively, the methanol-paraffin group exemplified more consistent cilia maximum intensities than the methanol-frozen group, which produced a few exceptional images but was not as consistent throughout the entirety of the group's samples.

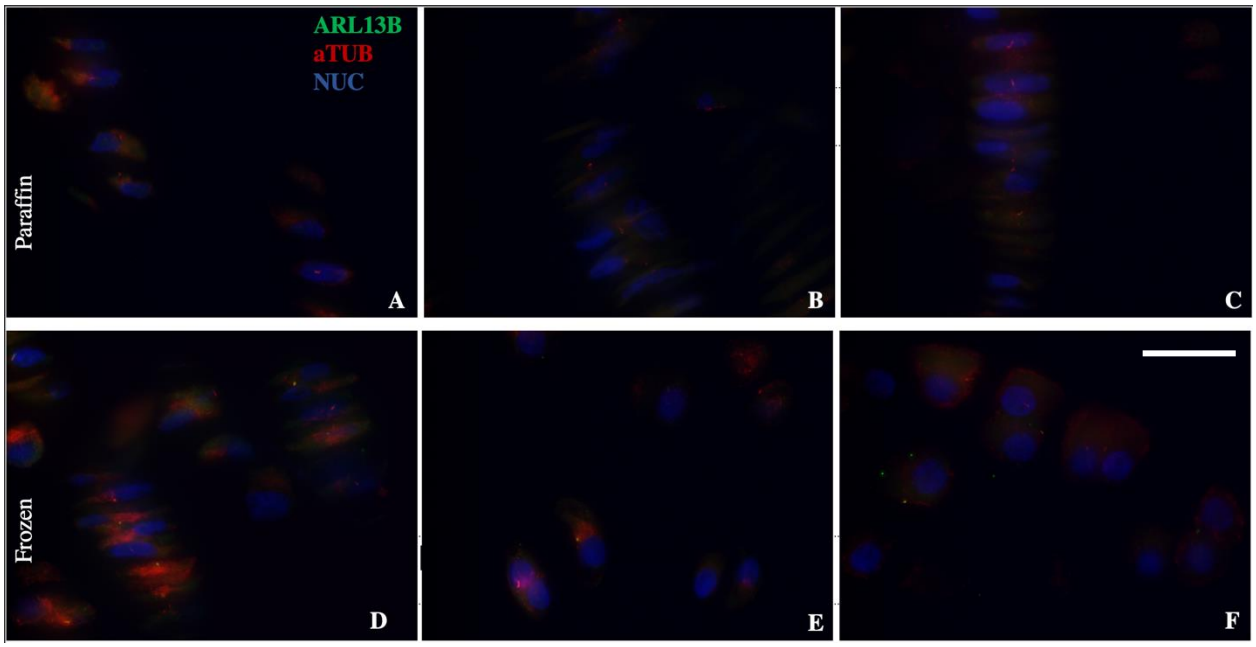

Figure 2. NBF-fixed cartilage samples from cadaveric swine. Panels A, B, and C were obtained from samples embedded in paraffin; panels D, E, and F were obtained from samples embedded in freezing medium. Cy3 was used to visualize acetylated alpha-tubulin (aTUB) primary antibody, shown in red. GFP was utilized to screen for ARL13B antibody, dyed green. DAPI was employed to stain cell nuclei, shown in blue. Contrast was enhanced to best distinguish primary cilia. (Scale bar = 20 μm)

Overall, the cilia in the NBF-fixed groups appeared less distinguished than in the methanol-fixed groups (Figure 2). While imaging cilia in the cartilaginous tissue, the faint appearance of the cilia sometimes blended in with nonspecific staining surrounding the cell bodies. Some images in the NBF-fixed groups displayed good contrast between the cilia and the background, as seen with aTUB. However, the ARL13b was often too faint to discover cilia. Since the ARL13b antibody was not used for analytic purposes, the difference between fixation methods for this stain was only observed from a qualitative

standpoint. The aTUB antibody provided better cilia staining than the ARL13b antibody for all four groups. The cilia in the samples treated with NBF-paraffin were not as bright as those in the NBF-frozen group. However, the NBF-paraffin group had less staining of the background or cell bodies, making cilia detection more effective than in the NBF-frozen group. For qualitative purposes we estimated the treatment groups should be ranked as follows, from overall highest to lowest quality; Me-P, Me-Fr, NBF-P, NBF-Fr.

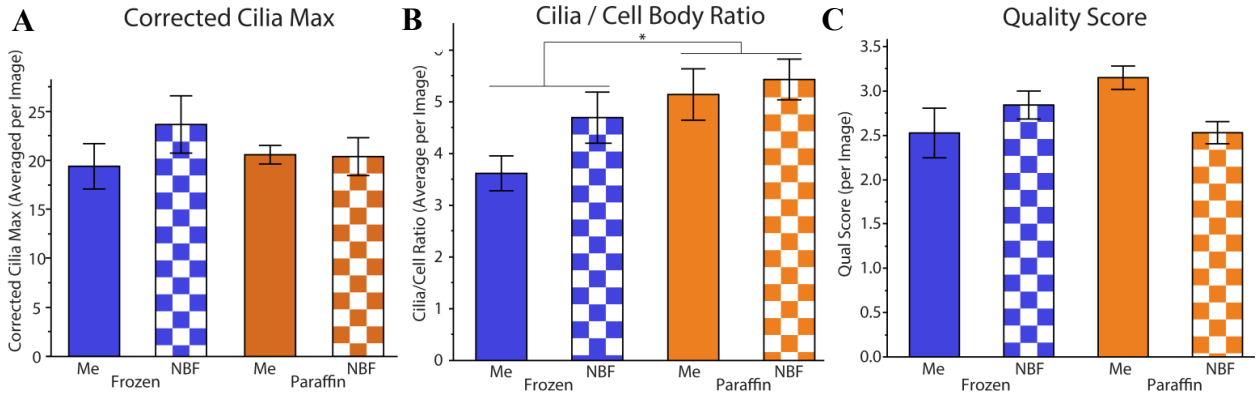

Figure 3. Graphs comparing the corrected cilia maximum intensity, the cilia maximum / cell body maximum ratio, and the image quality score by treatment type. (A) The corrected cilia maximum intensities for each cilia were averaged for each image and compared across treatment types, but did not show any significant differences. (B) The cilia maximum to cell body maximum ratio was calculated for each primary cilia, and then averaged for every image. When compared using ANOVA, a significant difference was detected between the paraffin and frozen embedding techniques. (C) The quality score for each image were averaged and compared across each treatment type, with no statistically significant differences identified. Asterisk (*) denotes significant differences derived from statistical analyses ($p < 0.05$). Graphs denote group mean ± standard error of the mean.

Quantitative measures of primary cilia staining are displayed as mean ± the standard error of the mean in Figure 3. No significant difference was found between the mean corrected cilia maximums of the different treatment groups, as determined by two-factor ANOVA ($p = 0.5181$). However, a significant difference in cilia/cell ratio was detected ($p = 0.0275$). The significant difference existed between the two embedding techniques, frozen and paraffin. The mean cilia/cell ratio of the frozen-embedded group was 4.16 ± 0.31 while mean cilia/cell ratio of the paraffin-embedded group was 5.29 ±

0.31. No significant difference in image qualitative score was found in the statistical analysis ($p = 0.0574$), but there was a trend towards Methanol/paraffin group performing the best. Indeed in the images, detection of cilia was often most apparent in this group, and the secondary cilia stain worked well in this treatment type.

Discussion

I was able to successfully view primary cilia in porcine cartilage tissue using both methanol and NBF fixation, as well as both frozen and paraffin sectioning. Fixation and microtomy were followed by antigen retrieval, which can be either heat- or proteolytic-induced. The antigen retrieval step of the IHC process is necessary to remove matrix proteoglycans and allow exposure of the antigen. Some studies recommend using testicular hyaluronidase to uncover cilia antigens in the tissue (McGlashan et al. 2006; Jensen et al. 2004); however, others utilized heat and sodium citrate buffer retrieval (Donnelly et al. 2010). Dr. Mohrman and I found success using heated-mediated antigen retrieval with sodium citrate buffer, although we did not compare with enzyme retrieval methods. As the dual-antibody staining method we used is often challenging, we first had to quickly decide on working dilutions for the two antibodies used to detect cilia: aTUB and ARL13b. We tried a series of dilutions of the antibodies both together and alone on the tissue to determine the lowest concentration of each that could be applied while still allowing detection of the primary cilia. The final concentrations of the primary antibodies were 1:1000 for aTUB and 1:200 for ARL13b. No data is included for this preliminary optimization as the criteria was more qualitative in nature.

Imaging with the multiphoton excitation microscope (MPE) proved challenging. During the imaging process, the MPE fires two photons which only excite a small area where the two photons meet, known as the focal plane. The MPE can excite and detect fluorescent emission at multiple wavelengths simultaneously, and has been used to visualize cilia in connective tissue (Donnelly et al. 2008). One advantage of using this type of microscope is that it allows for automated detection of tissue layers in the z-direction with minimal background noise. Since the primary cilia are small cellular structures that are oriented in various directions and in different z- planes of the sectioned tissue, we initially believed the MPE was the ideal method of capture. When using the MPE, we had difficulty capturing images of the cilia before the onset of photobleaching. With adjusted imaging technique, perhaps the MPE settings could have been optimized. However, for the purpose of this study, the upright epifluorescent microscope proved sufficient. We were able to obtain and compile images with the Cy3, GFP, and DAPI filters that accurately depict all potential cilia in field of view without bleaching the sample. Prior to obtaining images for analysis, the exposure time for each of the filters was adjusted to obtain the optimal settings for capturing cilia from all treatment groups. These settings remained constant for all images to avoid any possible variance in fluorescence intensity from image capture.

Of the two primary antibodies used for staining, only aTUB was analyzed for cilia intensity maximums, cilia / cell ratio, and quality score. ARL13b images were utilized to crosscheck for cilia position, however, no measurements were made for the ARL13b stain. Qualitatively, the methanol-fixed samples tended to display better ARL13b staining than those fixed in NBF (Figures 1 and 2). If using ARL13b antibody, I

hypothesize that methanol fixation would provide the most optimal cilia staining. Additional studies would need to be conducted to obtain analysis-based support for this prediction, rather than qualitative presumption.

Based on cilia fluorescence intensity (as judged by the cilia maximum intensity, Figure 3), the data did not show that any one treatment resulted in a significantly brighter staining of cilia. However, there was variability in the cilia intensity maximums, especially within the NBF-Fr treatment group (23.68 ± 2.13). As all images were captured on the same setting, it is improbable that the variation was due to imaging error. If the stain didn't turn out quite as pronounced on one slide as it did on another, there could be variability within the treatment group due to sectioning or staining methods. Obtaining data analysis from additional samples from each treatment group may help diminish variation within the groups and establish significant differences between treatment methods.

A significant difference was found between the two embedding techniques for the measure of cilia/cell intensity ratio, which was determined to be significantly greater in the paraffin than in the frozen-embedded group. No significant differences were found between fixation techniques. The ratio shows that there was a greater contrast between the cilia intensity and the cell body intensity with aTUB staining in the paraffin-embedded group, including tissues fixed in both methanol and NBF.

No significant difference was found between the qualitative scores of the images between treatment groups. The methanol-paraffin group had the highest mean qualitative score (3.15 ± 0.18), and qualitatively appeared to produce the best quality images in our observations. If given more time, it would be interesting to analyze a

greater sample size and note if the statistics support the Me-P group being capable of producing the highest quality images.

With paraffin-embedded tissue being the most desirable treatment for the optimization of cilia detection in growth plate tissue, particularly the proliferative zone, it would be interesting to test these four treatment types on other musculoskeletal tissues. Of particular interest to me would be tendons, iliotibial band/fascia, anterior and posterior cruciate ligaments. Due to time constraints, though other musculoskeletal tissues were collected, we were not able to utilize them for cilia staining. Analyzing more sections per treatment group and capturing more images may be more manageable with proper training and use of the multiphoton microscope. Instead of spending the time to capture and compile several images on a traditional upright microscope, the MPE is able to capture an image of all fluorescent labels and in multiple z-planes in one scan.

This staining optimization helped establish a ciliary visualization protocol in young, healthy swine so that we have a baseline for future clinical investigations. With the development of a suitable technique for cilia detection fin musculoskeletal tissue, Dr. Mohrman has begun to use the conclusions of our experiments when staining human tissue specimens (data not shown). As patient samples can be difficult to obtain, our work helps ensure the human specimens are not wasted with non-working staining protocols.

Conclusion

Comparing various fixation and embedding methods in an IHC protocol of cadaveric swine growth plate tissue showed trends in favor of the Me-P method for optimal cilia detection. Statistical results supported Paraffin-embedding as the optimal method for the generation of the highest cilia / cell ratio. The most efficient and reliable method for cilia visualization is desired as it aids in the understanding of cilia and its corresponding functional role in musculoskeletal tissue. Several studies note a direct correlation between the primary cilium and growth plate development. With the optimization of staining methods and microscopy techniques, the primary cilium has the potential to become the target of therapeutic drugs to treat growth plate disorders.

Acknowledgements

Special thank you to Dr. Ashley Mohrman for her contributions, investment, and support throughout this research project, beginning in the Spring of 2018. Dr. Mohrman served as a mentor in supporting my research endeavors. I'd like to acknowledge Akron Children's Hospital for organizing CITI training and for allowing the use of their laboratory and equipment. I'd also like to acknowledge the Institutional Animal Care and Use Committee of Northeast Ohio Medical University for providing permission to collect and utilize tissue samples from cadaveric swine. Thank you to Northeast Ohio Medical University for allowing the use of the multiphoton excitation microscope. Thank you to Dr. Jordan Renna for his guidance regarding the modification of antigen retrieval methods and immunohistochemistry protocol.

References

Deren, M. E., Xu, Y., Yingjie, G., & Qian, C. (2016). Biological and Chemical Removal of Primary Cilia Affects Mechanical Activation of Chondrogenesis Markers in Chondroprogenitors and Hypertrophic Chondrocytes. International Journal Of Molecular Sciences, 17(2), 1-10. doi:10.3390/ijms17020188

Donnelly, E., Ascenzi, M., & Farnum, C. (2010). Primary cilia are highly oriented with respect to collagen direction and long axis of extensor tendon. Journal Of Orthopaedic Research, 28(1), 77-82. doi:10.1002/jor.20946

Donnelly, E., Williams, R., & Farnum, C. (2008). The Primary Cilium of Connective Tissue Cells: Imaging by Multiphoton Microscopy. The Anatomical Record: Advances in Integrative Anatomy and Evolutionary Biology, 291(9), 1062-1073. doi:10.1002/ar.20665

Garrison, P., Yue, S., Hanson, J., Baron, J., & Lui, J. C. (2017). Spatial regulation of bone morphogenetic proteins (BMPs) in postnatal articular and growth plate cartilage. Plos ONE, 12(5), 1-18. doi:10.1371/journal.pone.0176752

Ho, L., Ali, S. A., Al-Jazrawe, M., Kandel, R., Wunder, J. S., & Alman, B. A. (2012). Primary cilia attenuate hedgehog signalling in neoplastic chondrocytes. Oncogene, 32(47), 5388-5396. doi:10.1038/onc.2012.588

IHC/ICC Sample Fixation (Formalin vs. Alcohol). (n.d.). Retrieved from https://www.novusbio.com/sample-fixation-for-ihc-icc

Ikeda, M., Imaizumi, M., Yoshie, S., Otsuki, K., Miyake, M., Hazama, A., . . . Omori, K. (2016). Regeneration of tracheal epithelium using mouse induced pluripotent stem cells. Acta Oto-Laryngologica, 136(4), 373-378. doi:10.3109/00016489.2015.1121548

Immunohistochemistry Introduction. (n.d.). Retrieved from http://www.ihcworld.com/_intro/intro.htm

Jensen, C., Poole, C., McGlashan, S., Marko, M., Issa, Z., Vujcich, K., & Bowser, S. (2004). Ultrastructural, tomographic and confocal imaging of the chondrocyte primary cilium in situ. Cell Biology International, 28(2), 101. doi:10.1016/j.cellbi.2003.11.007

Lavagnino, M. (2016). Hypoxia inhibits primary cilia formation and reduces cell-mediated contraction in stress-deprived rat tail tendon fascicles. Muscles, Ligaments and Tendons Journal. doi:10.11138/mltj/2016.6.2.193

Mackie, E., Tatarczuch, L., Mirams, M. (2011). The skeleton: a multi-functional complex organ. The growth plate chondrocyte and endochondral ossification. Journal Of

Endocrinology, 211(2), 109-121.

Mcglashan, S. R., Jensen, C. G., & Poole, C. A. (2006). Localization of Extracellular Matrix Receptors on the Chondrocyte Primary Cilium. Journal of Histochemistry & Cytochemistry,54(9), 1005-1014. doi:10.1369/jhc.5a6866.2006

Moore, E. R., & Jacobs, C. R. (2018). The primary cilium as a signaling nexus for growth plate function and subsequent skeletal development. Journal Of Orthopaedic Research, 36(2), 533-545. doi:10.1002/jor.23732

Schimmack, S., Kneller, S., Dadabaeva, N., Bergmann, F., Taylor, A., Hackert, T., & ... Strobel, O. (2016). Epithelial to Stromal Re-Distribution of Primary Cilia during Pancreatic Carcinogenesis. Plos ONE, 11(10), 1-16. doi:10.1371/journal.pone.0164231

Yuan, X., Serra, R. A., & Yang, S. (2015). Function and regulation of primary cilia and intraflagellar transport proteins in the skeleton. Annals Of The New York Academy Of Sciences, 1335(1), 78-99. doi:10.1111/nyas.12463

Yuan, X., & Yang, S. (2015). Deletion of IFT80 Impairs Epiphyseal and Articular Cartilage Formation Due to Disruption of Chondrocyte Differentiation. Plos ONE, 10(6), 1-19. doi:10.1371/journal.pone.0130618